Figure **S.1** shows the ^{1}H NMR spectrum of DPA_8OS, **1a**. The nine aromatic protons are accounted for through the integration of the five overlapping multiplets, accounting for nine protons. The largest downfield shift is 7.71 ppm, which is between the predictions of 7.6 and 8.2 ppm for the CF_3 and NO_2 substituted diphenylacetylene derivatives calculated using the "ChemBioDraw Ultra" software package.[68] One interpretation of this data is that the silsequioxane cage is slightly more electron withdrawing than a CF_3 group.

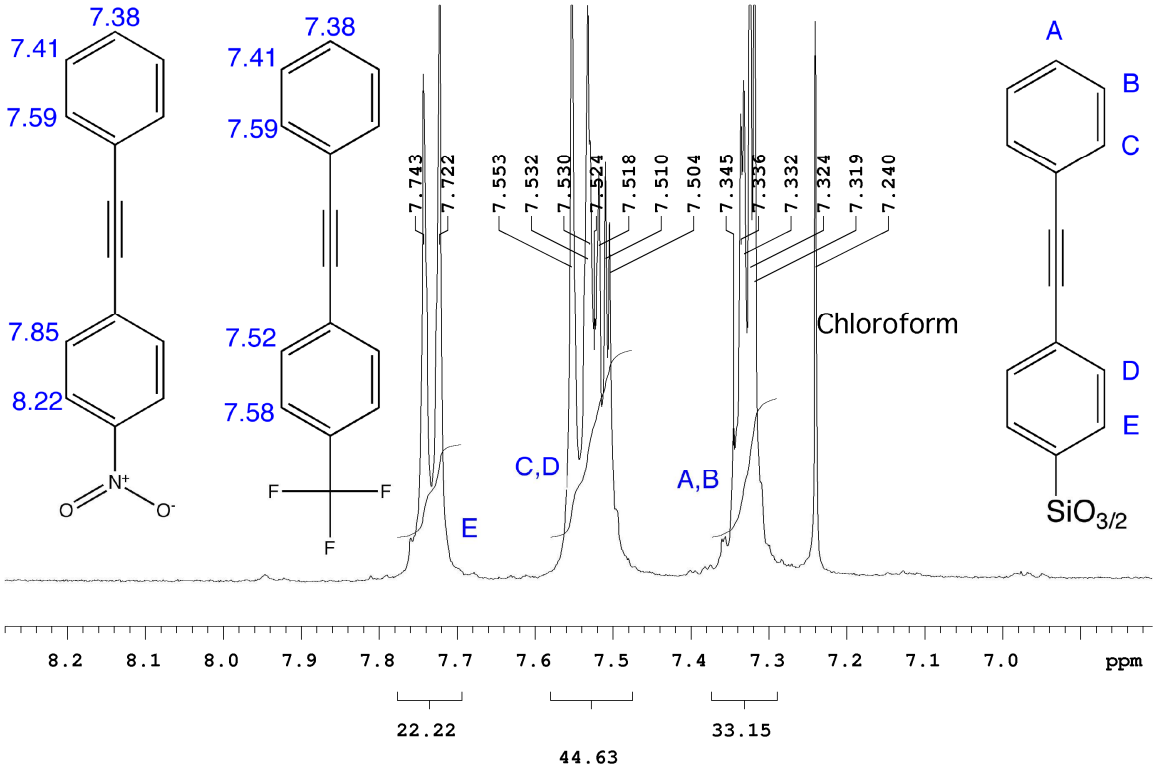

Figure S.1. ^{1}H NMR spectrum of the DPA_8OS in $CDCl_3$.

Figure **S.2** shows the ^{13}C NMR spectrum of DPA_8OS. Eight peaks are detected in the aromatic region, representing the eight different carbon species. The larger four peaks correspond to carbons bonded to hydrogen, which are enhanced by proton decoupling. The largest downfield shift is 134 ppm, which is between the predictions of 133 and 148

ppm for the CF_3 and NO_2 substituted diphenylacetylene derivatives. Again, one interpretation of this data is that the silsesquioxane cage is slightly more electron withdrawing than a CF_3 group.

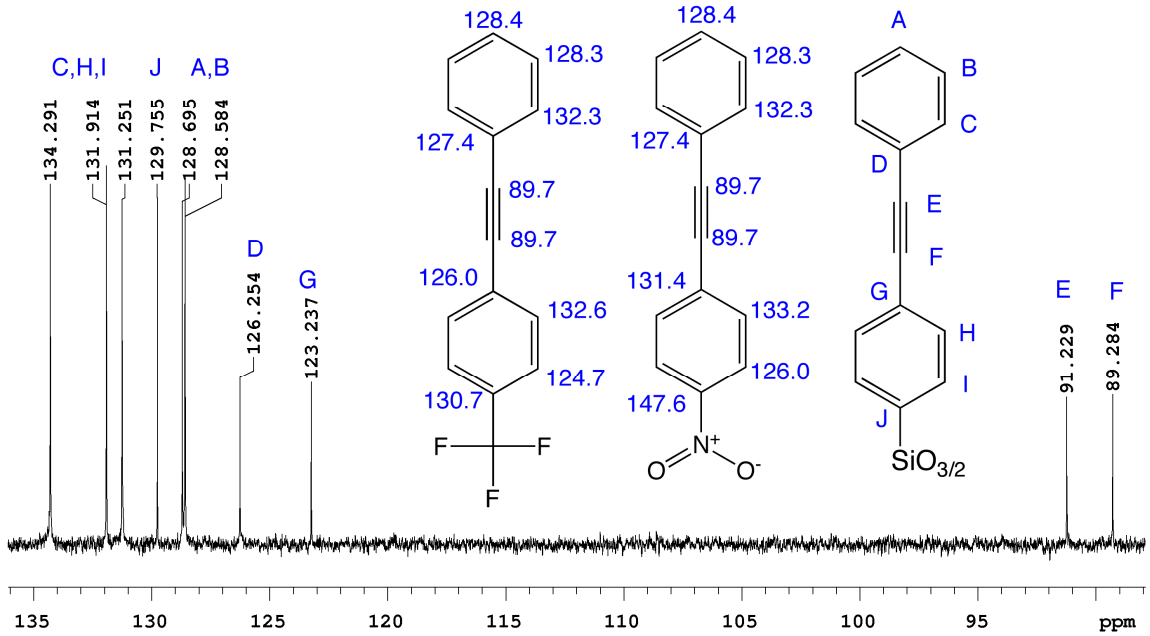

Figure S.2. ^{13}C NMR spectrum of DPA_8OS in $CDCl_3$.[68]

Figure **2** shows the MALDI-TOF spectrum of DPA_8OS. The large peak corresponds to the single silver adduct of the octameric product. The small peak at 1832.8 Da corresponds to the octamer without a silver adduct and the small peak at 1840.7 Da represents the silsesquioxane cage compound with seven diphenylacetylene corners and one phenyl corner.

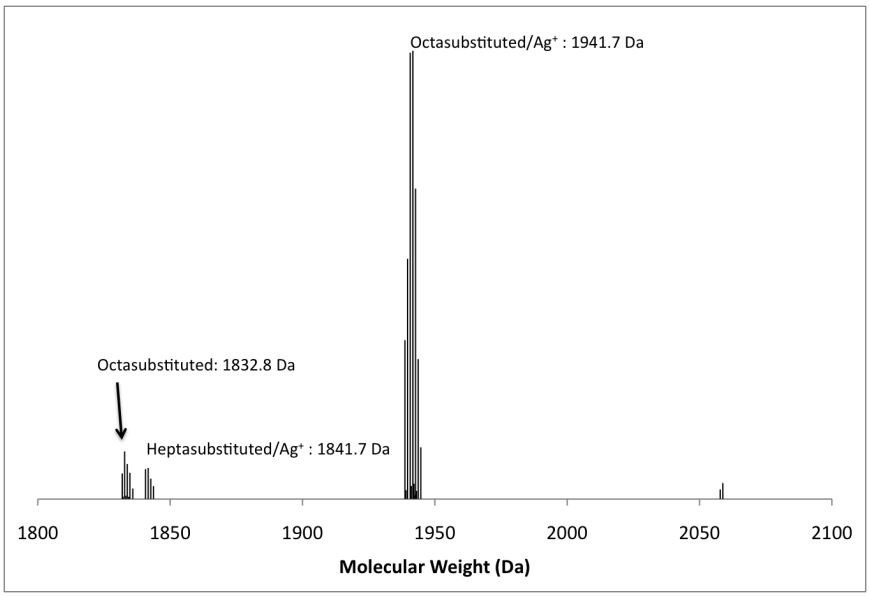

Figure S.3. MALDI-TOF spectrum of DPA_8OS (Ag^+/Dithranol).

Figure **S.4** shows the ^1H NMR spectra of the (*p*-Tolylethynyl-Phenyl)$_8$OS, **1b**. The eight aromatic protons are detected as four well separated multiplets. The methyl protons are found at 2.39 ppm. The integration of the methyl protons to the aromatic protons is 28%, close to the theoretical 27 % for the symmetric compound. Figure **S.5** shows the ^{13}C NMR spectrum of (*p*-Tolylethynyl-Phenyl)$_8$OS. Eight peaks are detected in the aromatic region, representing the eight different carbon species.

Figure **S.6** shows the MALDI-TOF spectrum of (*p*-Tolylethynyl-Phenyl)$_8$OS. The large peak corresponds to the single silver adduct of the octameric product. The small peak at 1944.9 Da corresponds to the octamer without a silver adduct. The small peak at 1938.7 Da corresponds to the silsesquioxane cage compound with seven tolylphenylacetylene corners and one phenyl corner with a silver adduct. The small peak at 2053.7 Da indicates the silsesquioxane cage compound with eight tolylphenylacetylene corners and one corner with an additional tolylacetylene unit with a silver adduct.

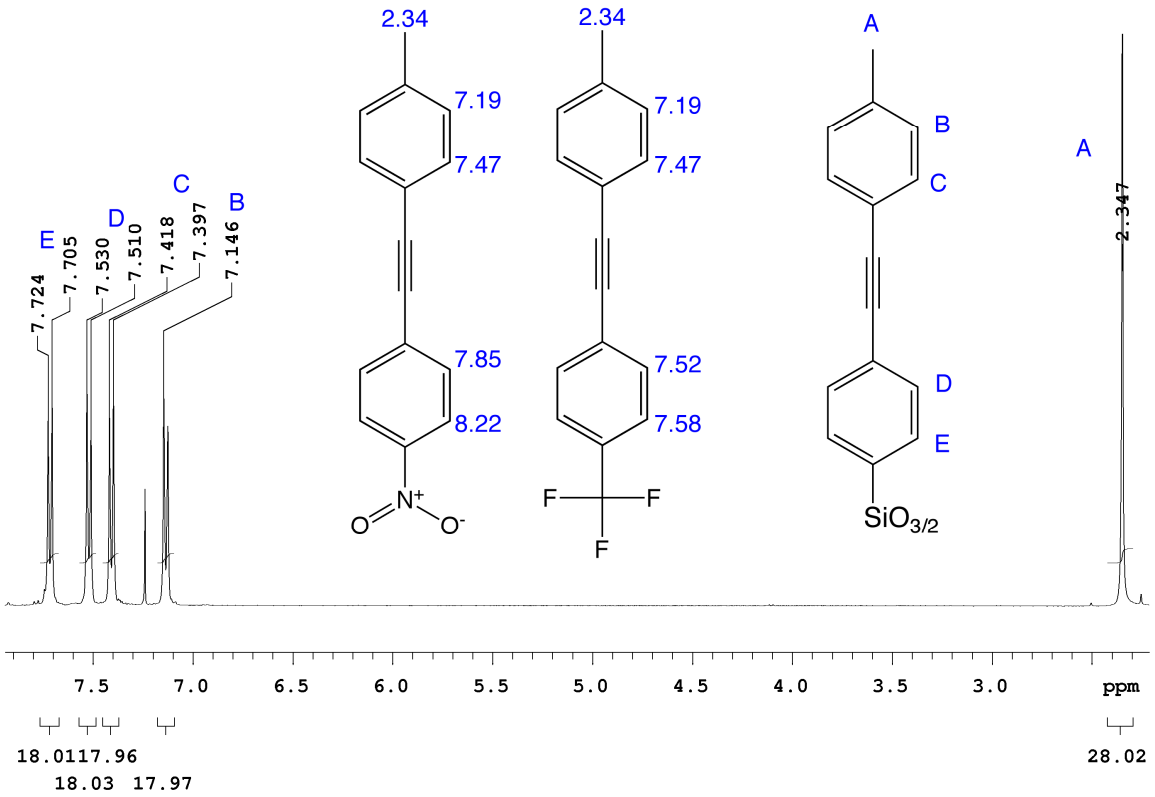

Figure S.4. ^{1}H NMR spectrum of (*p*-Tolylethynyl-Phenyl)$_8$OS in $CDCl_3$.

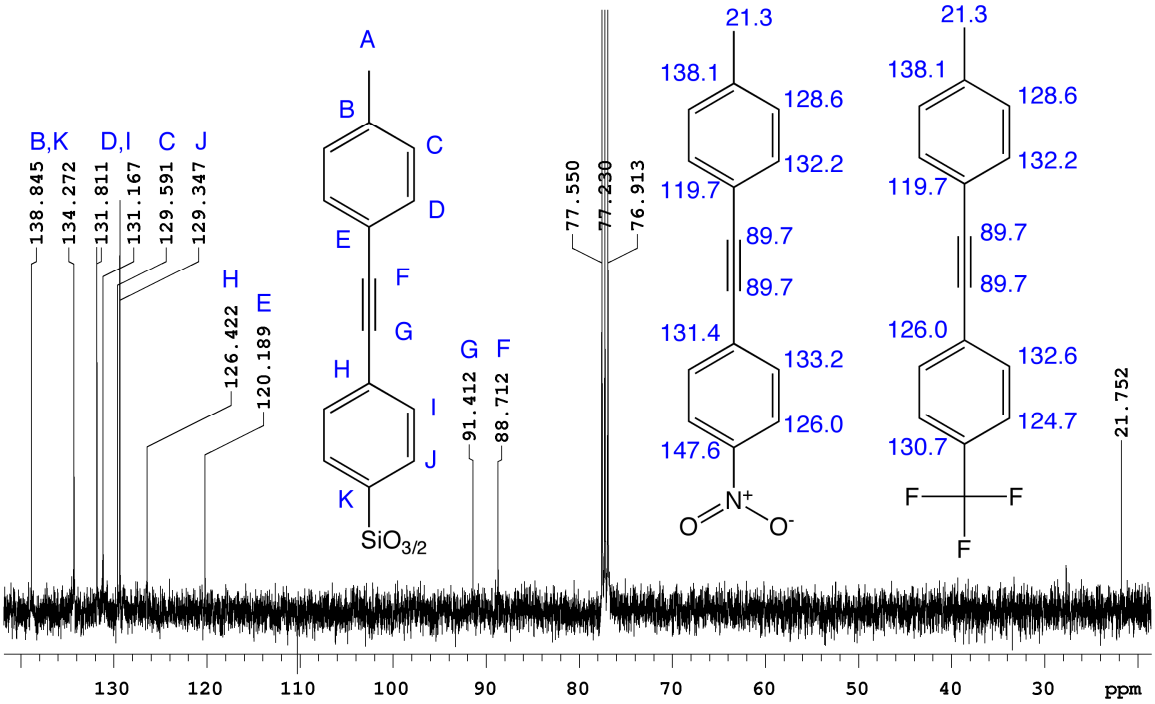

Figure S.5. ^{13}C NMR spectrum of (*p*-Tolylethynyl-Phenyl)$_8$OS in $CDCl_3$.

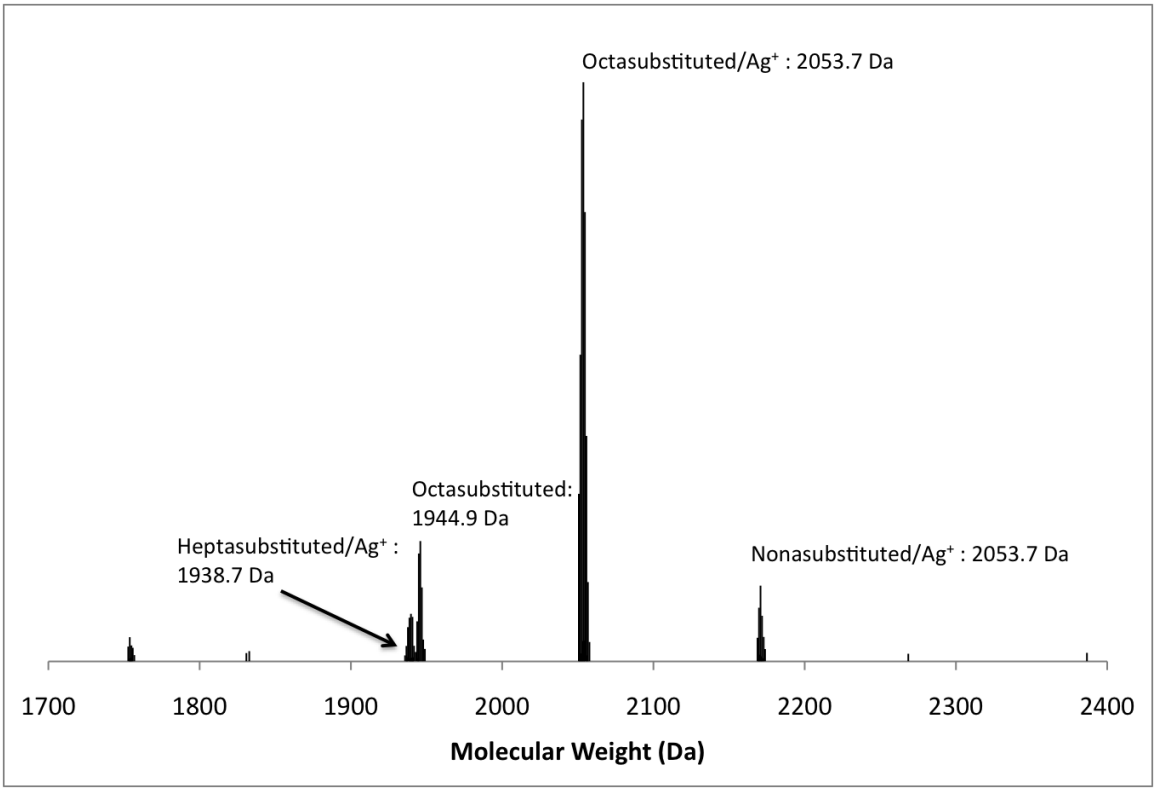

Figure S.6. MALDI-TOF spectrum of the (*p*-Tolylethynyl-Phenyl)$_8$OS (Ag^+/Dithranol).

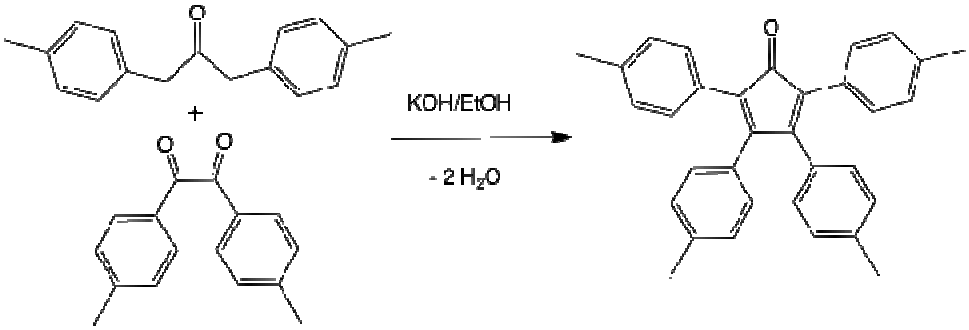

Scheme S.1 Synthesis of tetra-*p*-tolylcyclopentadienone.

The as-synthesized tetra(*p*-tolyl)cyclopentadienone is essentially pure by ^{1}H NMR, but may be recrystallized by the addition of an equivalent volume of methanol to a hot, saturated toluene solution of the tetracyclone. The ^{1}H NMR spectrum of the product is shown in Figure **S.7**.

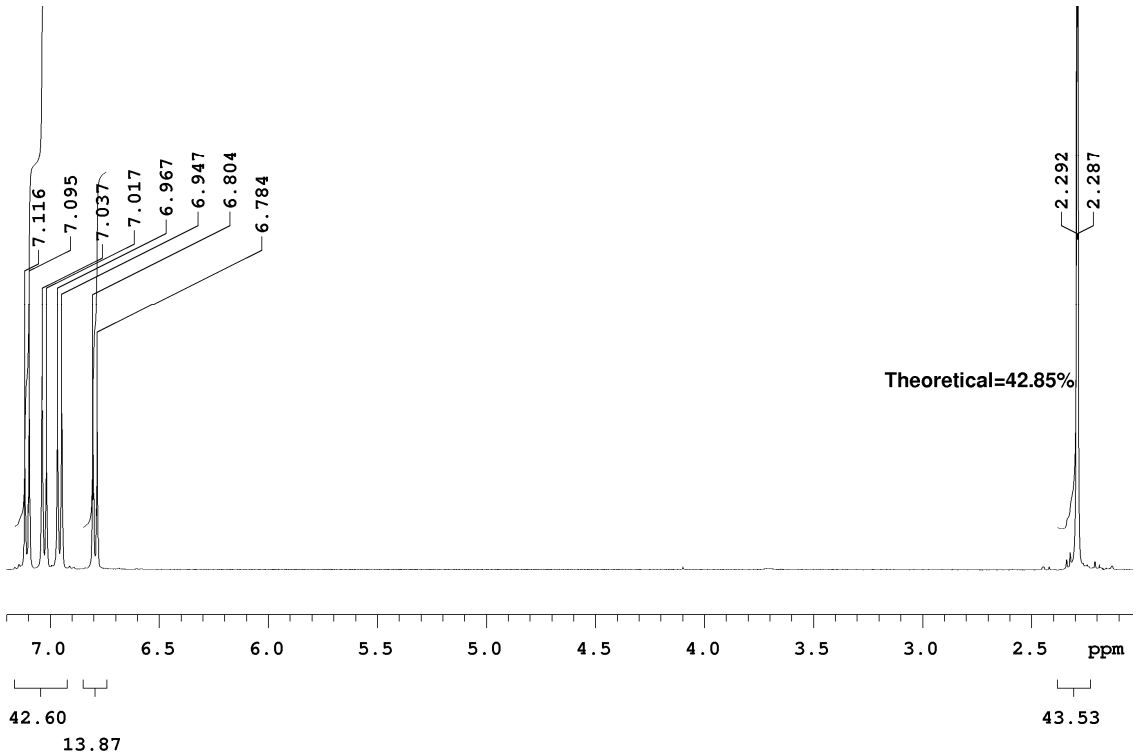

Figure S.7 ^{1}H NMR of tetra(*p*-tolylcyclopentadienone in $CDCl_3$.

Figure **S.8** shows the ^{1}H spectrum of $(Ph_6C_6)_8OS$. The aromatic resonance are found between 6 and 7 ppm, consistent with the single proton resonance of hexaphenylbenzene at 6.8 ppm. The breadth of the peaks may be due to a reduced tumbling rate in solution, which leads to line broadening. The presence of two peaks indicates the presence of two distinct chemical environments. Presumably this is due to the interaction of the electron-withdrawingsilsesquioxane cage with adjacent aromatic rings.

Figure **S.9** shows the ^{13}C spectrum of $(Ph_6C_6)_8OS$, with thirteen resolved peaks, which correspond well to the reported shifts: "δ 140.5, 140.2 (s, quaternary), 131.3, 126.4, 125.0 ppm (s, C_6H_5)". The relatively narrow peaks suggest that a reduced tumbling rate may not account for the breadth of the ^{1}H NMR peaks.

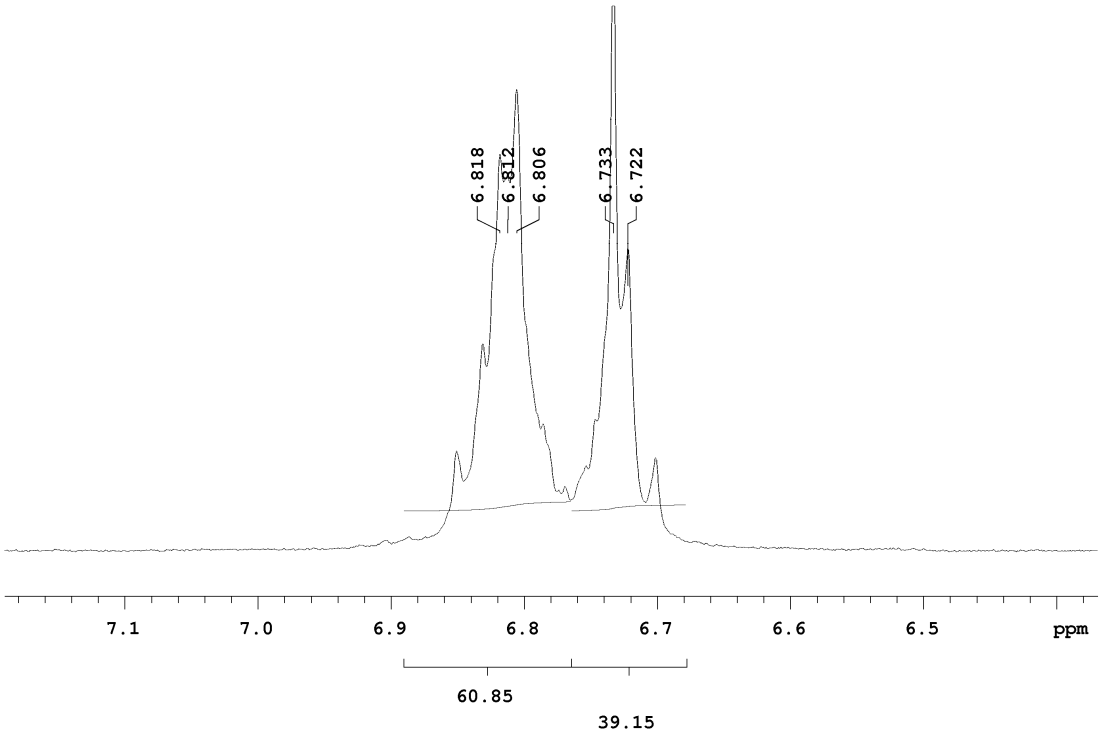

Figure S.8 ^{1}H spectrum of $(Ph_6C_6)_8OS$ in $CDCl_3$.

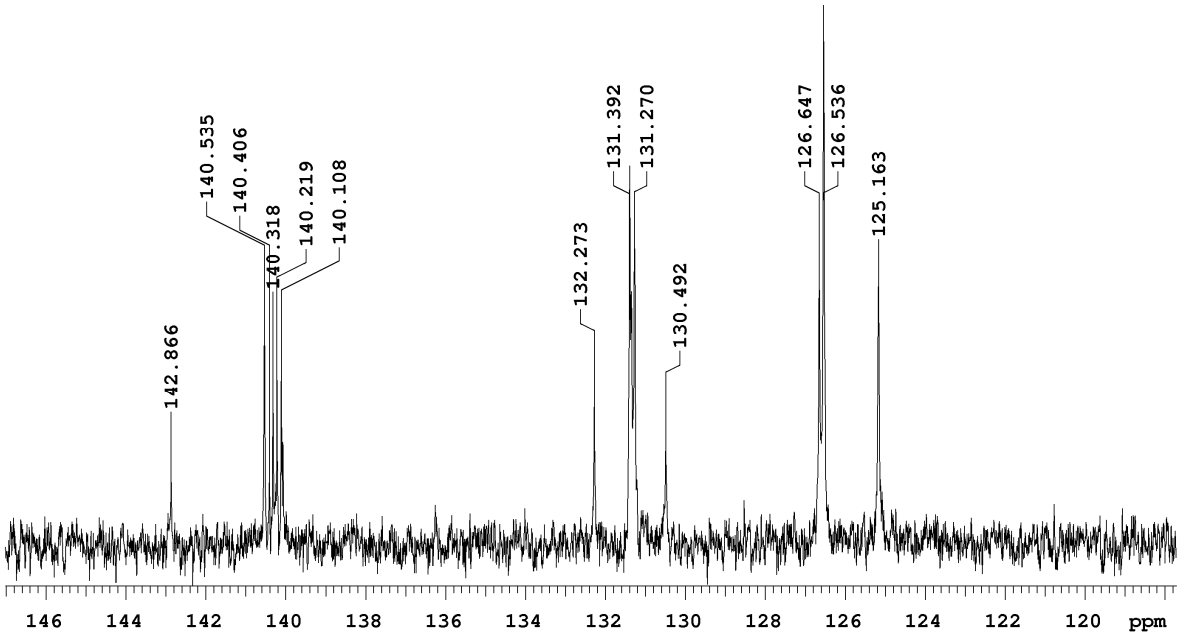

Figure S.9 ^{13}C spectrum of the $(Ph_6C_6)_8OS$ in $CDCl_3$.

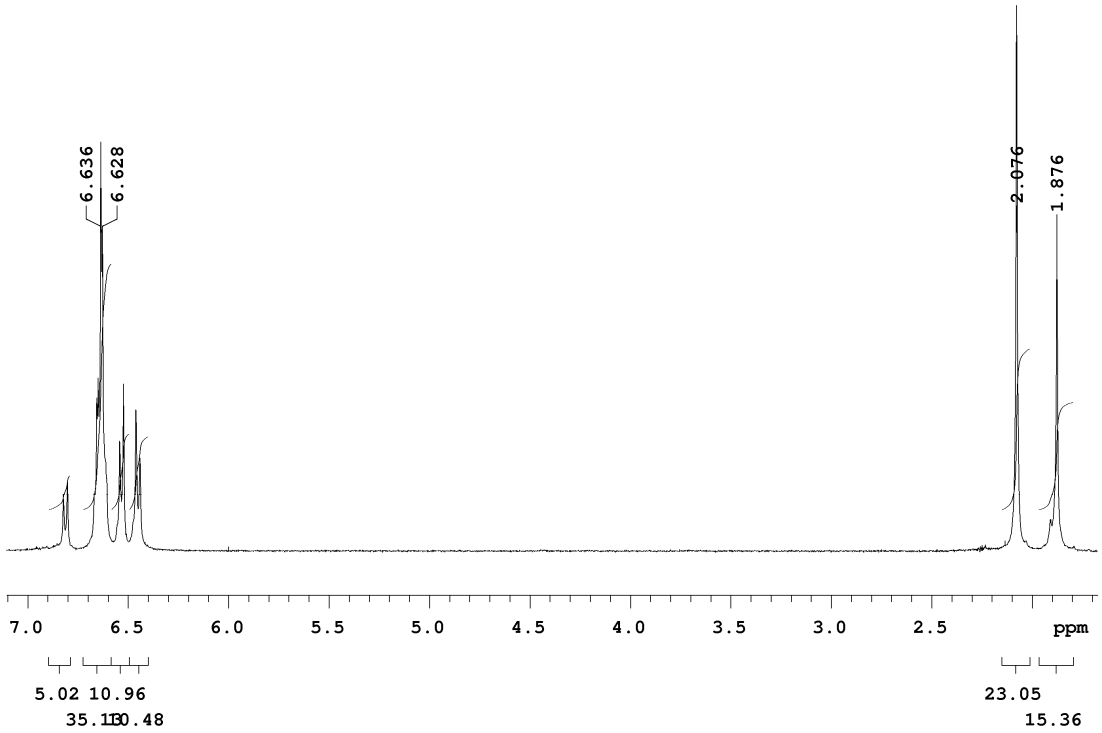

Figure S.10. ^{1}H spectrum of the (p-Tolyl$_5$PhC$_6$)$_8$OS in CDCl$_3$.
Ar-H vs. CH$_3$ Integrations: Ar-H expected 61.6%, found 61.5%

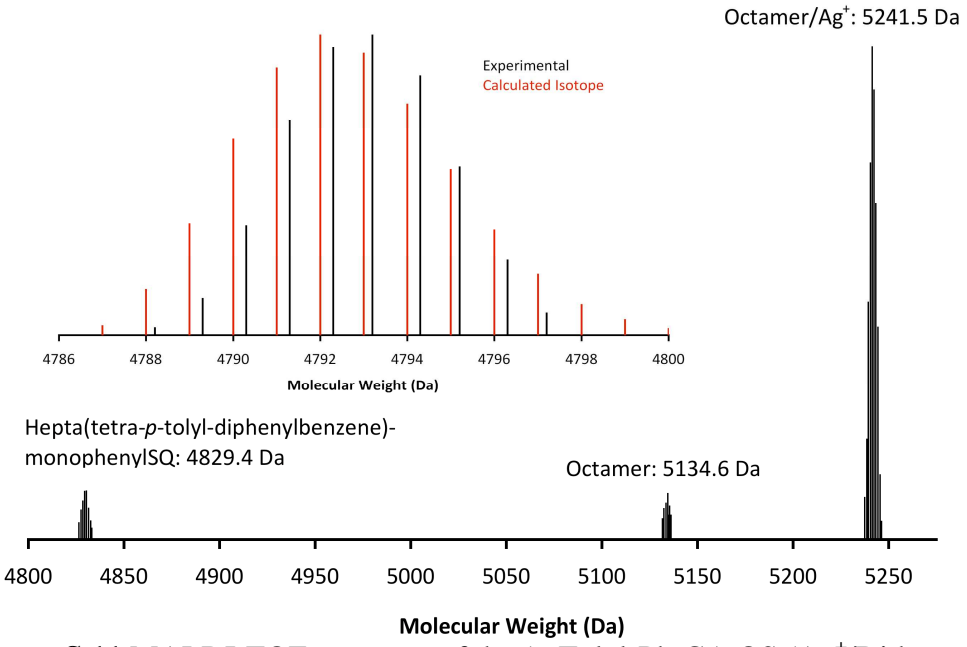

Figure S.11 MALDI-TOF spectrum of the (p-Tolyl$_4$Ph$_2$C$_6$)$_8$OS (Ag$^+$/Dithranol).

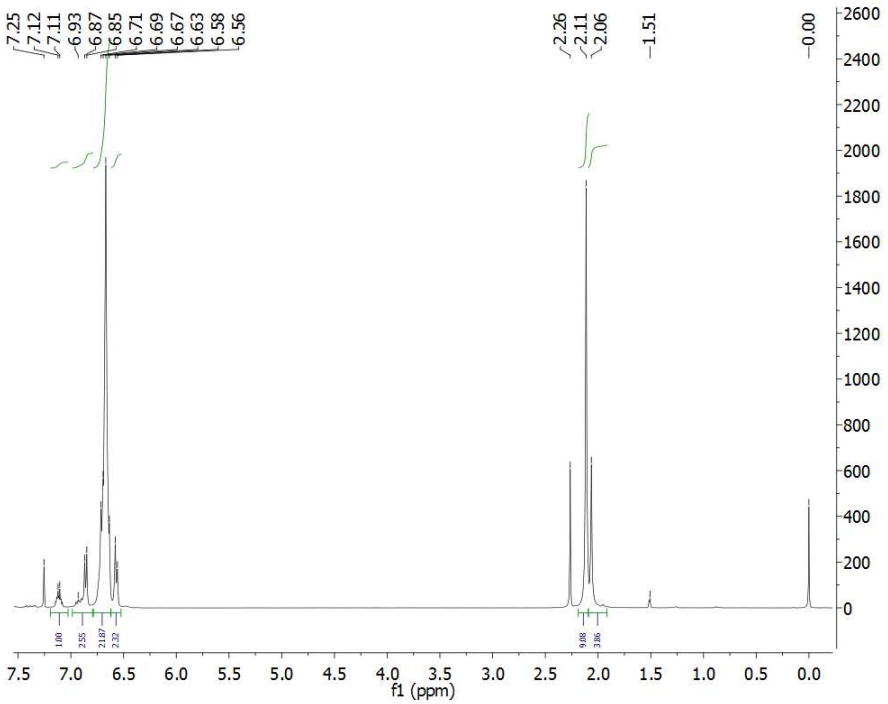

Figure S.12. ^{1}H spectrum of the (p-Tolyl$_4$Ph$_2$C$_6$)$_8$OS in CDCl$_3$. Peak at 2.26 ppm attributable to residual acetone. Ar-H vs. CH$_3$ Integrations: Ar-H Integrations: expected 67.6%, found 68.3%

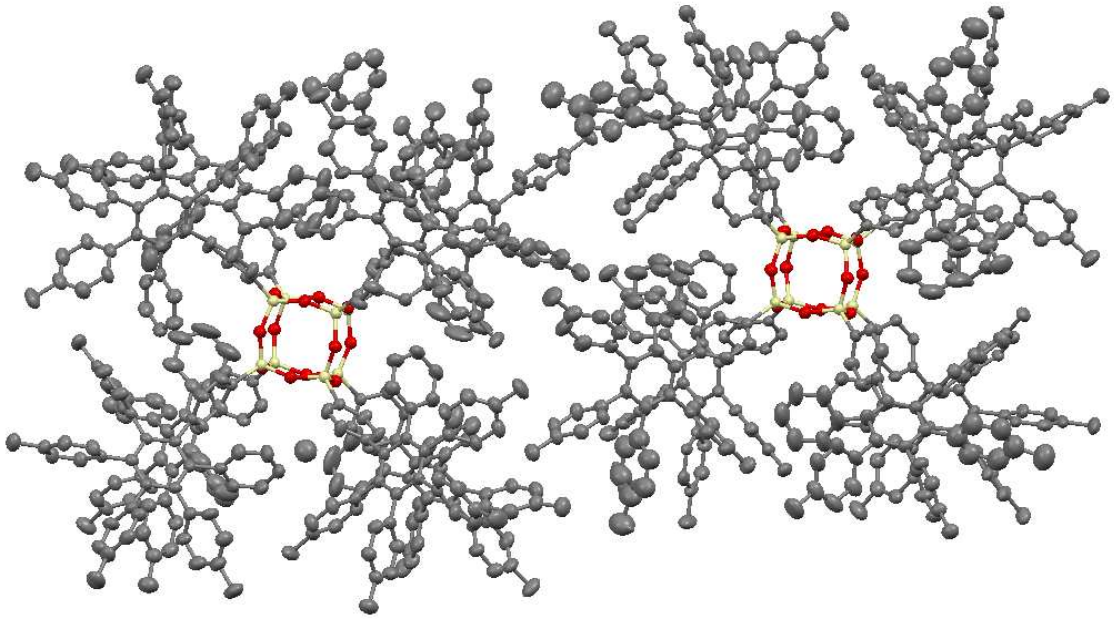

Figure S.13. Asymmetric unit of the (p-Tolyl$_4$Ph$_2$C$_6$)$_8$OS crystal structure.

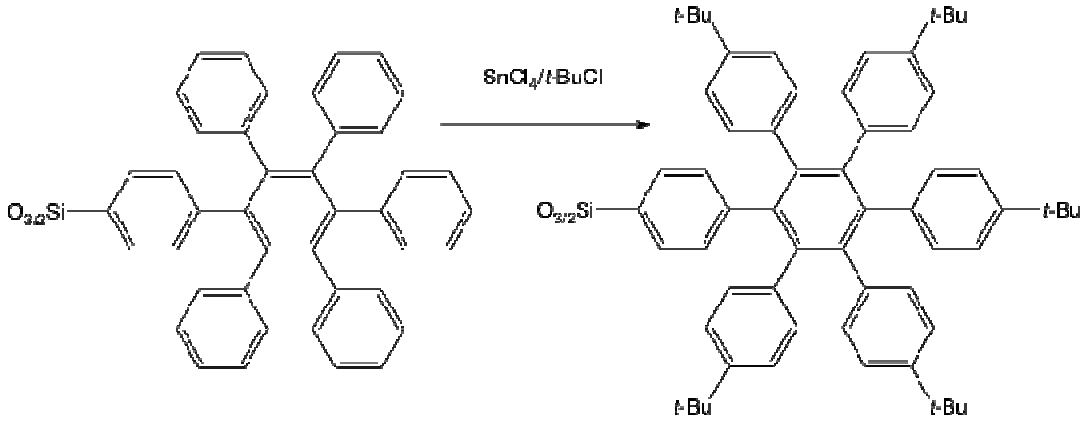

Scheme S.2 *t*-Butylation of $(Ph_6C_6)_8OS$.

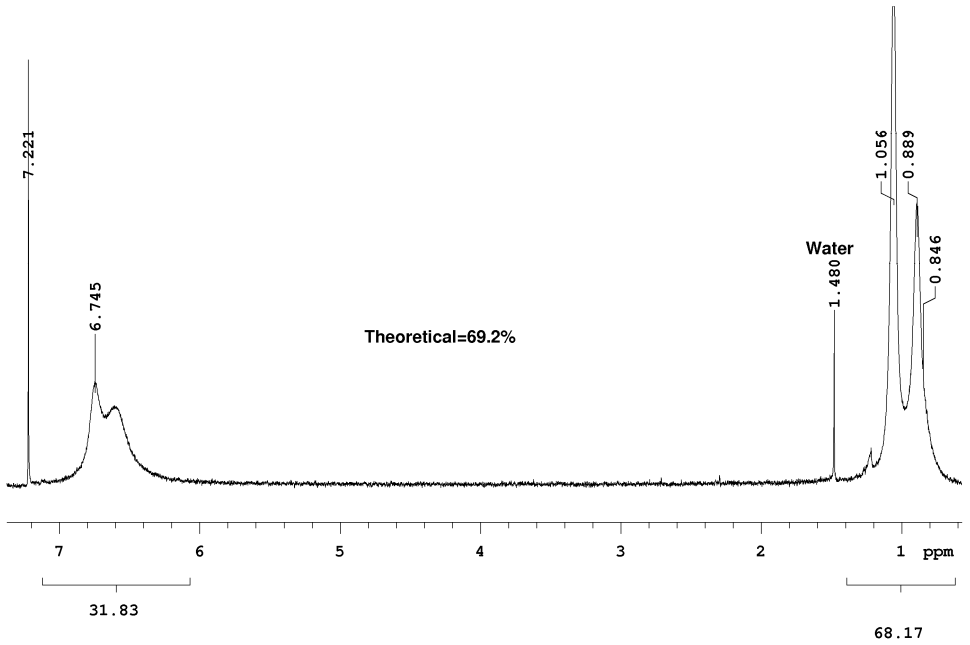

Figure S.14 ^{1}H spectrum of the t-butylated $(Ph_6C_6)_8OS$ in $CDCl_3$.

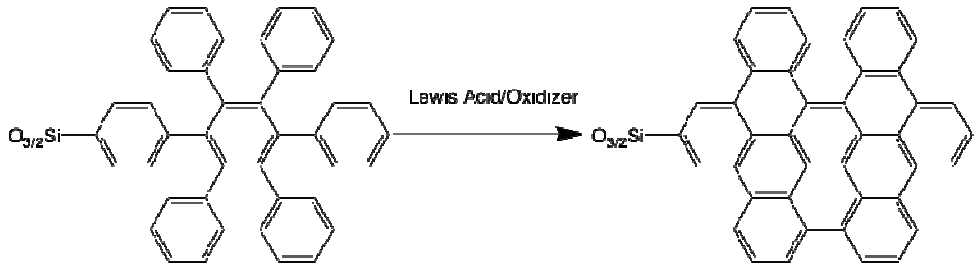

Scheme S.3 Scholl-type dehydrogenative cyclization.

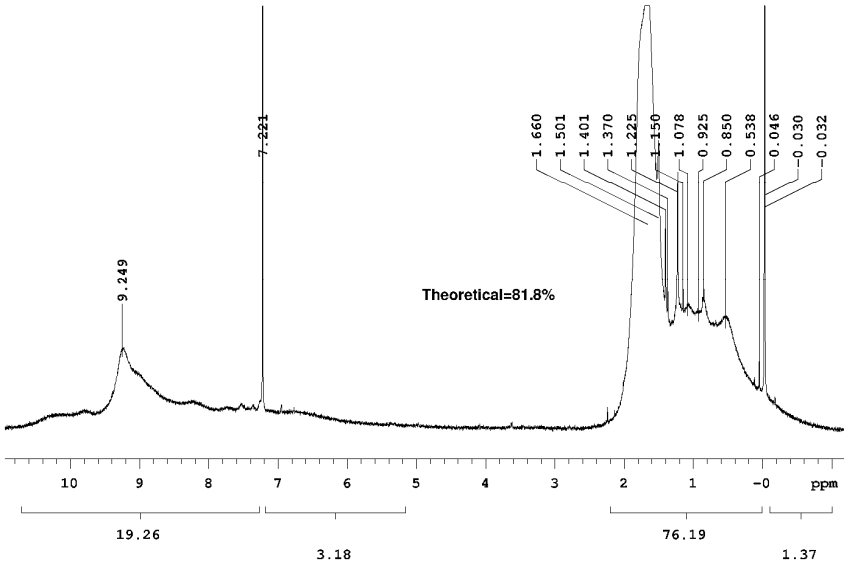

Figure S.15 ^{1}H spectrum of the cyclized, *t*-butylated $(Ph_6C_6)_8OS$ in $CDCl_3$.

The FTIR spectrum of this compound is shown in Figure **17**. The presence of the ν Si-O-Si bands of the silsesquioxane core are seen from 1200-1000 cm^{-1}, and the vibrational contributions of the aromatic rings can be seen at 3061 (ν ArC-H), 1575-1500 (ν/δ C-C), and 700 (δ C-H) cm^{-1}. Scaled to equivalent heights of the ν Si-O-Si bands, decreases in the ν ArC-H (3100-3000 cm^{-1}) bands suggest the loss of aromatic protons in the cyclization reaction. Additionally, peaks in the fingerprint region, (2000-1600 cm^{-1}) decrease, as well as a significant decrease in the intensity of the peak at 575 cm^{-1}.

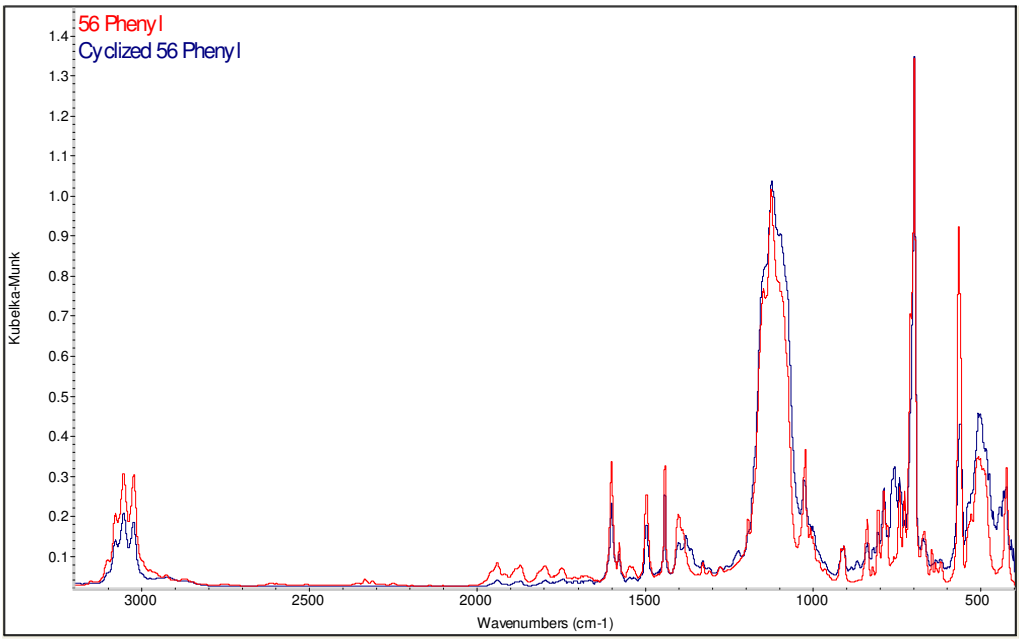

Figure S.16 FTIR spectra of the $(Ph_6C_6)_8OS$ and its cyclization product, 3200-400cm^{-1}.

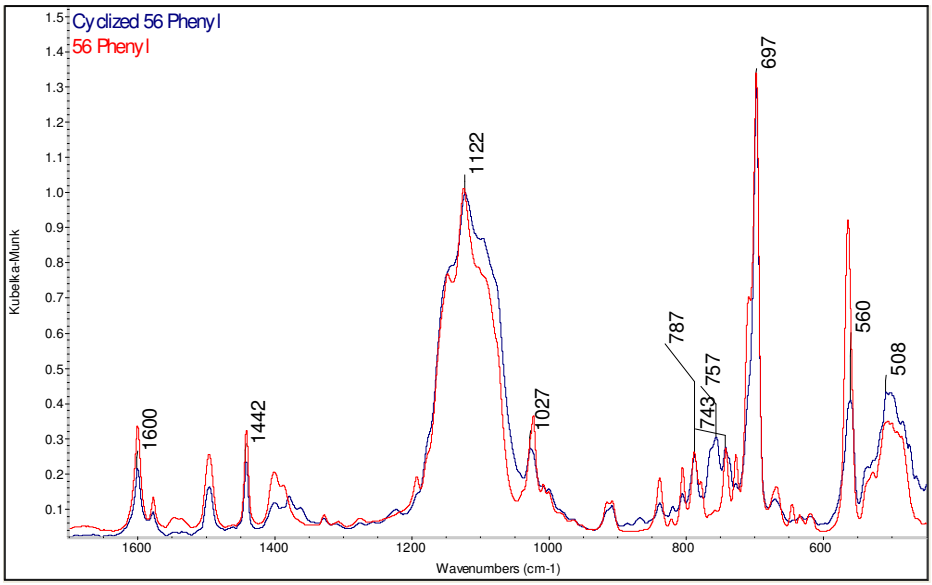

Figure S.17 FTIR spectra of the $(Ph_6C_6)_8OS$ and its cyclization product, 1700-400 cm^{-1}.

The FTIR spectrum of this compound is shown in Figure **18**. The presence of the ν Si-O-Si bands of the silsesquioxane core are seen from 1200-1000 cm^{-1}, and the vibrational contributions of the aromatic rings can be seen at 3061 (ν ArC-H) and 2915 (ν Bz-H), 1575-1500 (ν/δ C-C), and 850-750 (δ C-H) cm^{-1}.

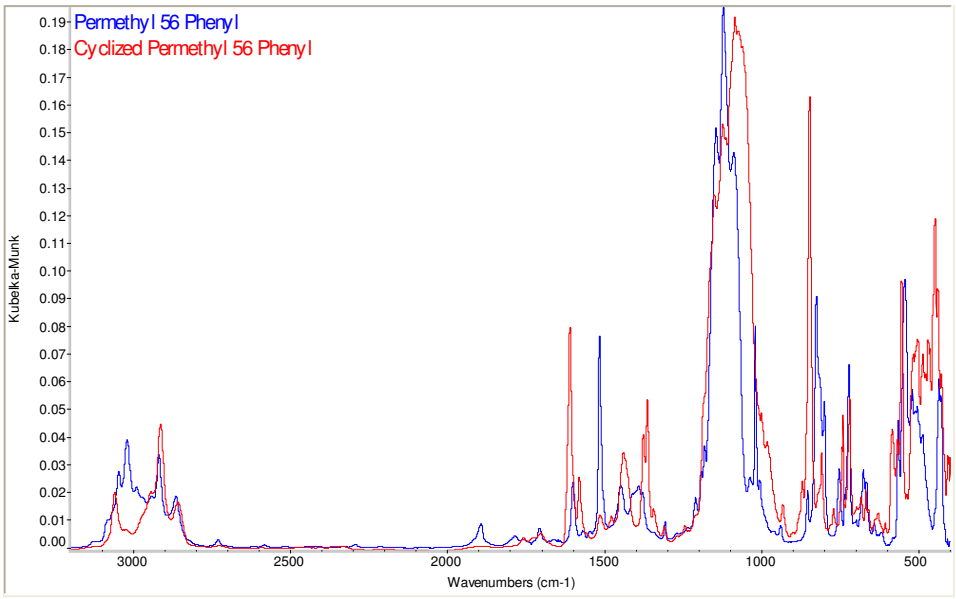

Figure S.18 FTIR spectra of the $(p\text{-Tolyl}_5\text{PhC}_6)_8\text{OS}$ and its cyclization product, 3200-450 cm^{-1}.

Several pronounced differences are seen in this case. A dramatic decrease in the ν ArC-H bands (3100 tot 3000 cm^{-1}), which is consistent with a loss of aromatic protons. The absorbance at 1525 cm^{-1} decreases dramatically, and the intensity of the peak at 1600 cm^{-1} strongly increases. New peaks at 1350-1400 cm^{-1} arise, and peak shift from 840 to 850 cm^{-1} is seen. Finally the absorbance of the ν Si-O-Si bands broadens and shifts from 1075 to 1025 cm^{-1}.

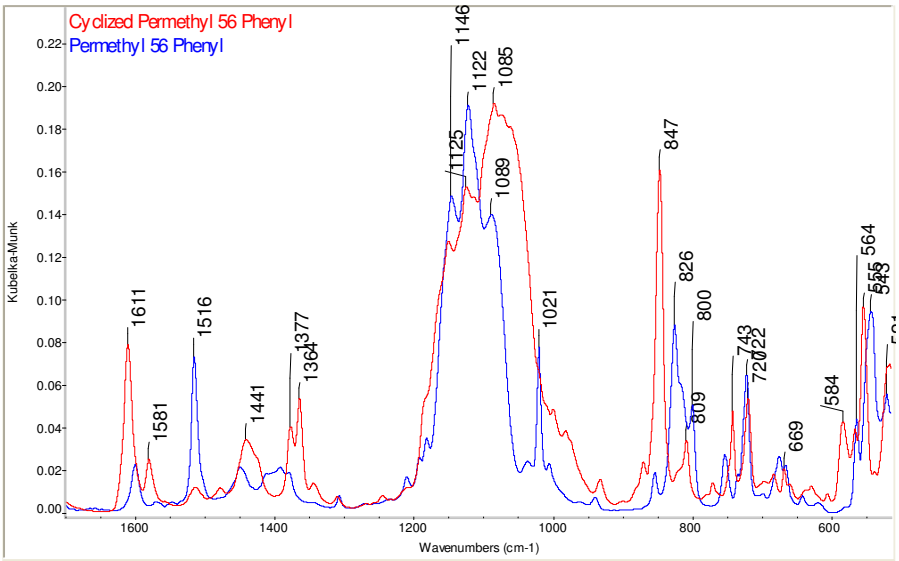

Figure S.19 FTIR spectra of the (p-Tolyl$_5$PhC$_6$)$_8$OS and its cyclization product, 1700-500 cm^{-1}.